Hydrogen gas inhibits lung cancer progression through targeting SMC3

Dongchang Wang, Lifei Wang, Yu Zhang, Yunxia Zhao, Gang Chen*

Department of Respiration, The Third Hospital of Hebei Medical University, Shijiazhuang, Hebei, China

ARTICLE INFO

ABSTRACT

Lung cancer is one of the most common lethal malignancies in the globe. The patients' prognoses are dim due to its high metastatic potential and drug resistance. Therefore, in the present study, we aim to find a more potent therapeutic approach for lung cancer. We mainly explored the function of hydrogen gas (H_2) on cell viability, apoptosis, migration and invasion in lung cancer cell lines A549 and H1975 by CCK-8, flow cytometry, wound healing and transwell assays, respectively. We used RNA-seq, qPCR and western blotting to detect the different expression genes (DEGs) between H_2 group and control group to find the gene related to chromosome condensation. Besides, we confirmed the structural maintenance of chromosomes 3 (SMC3) and H_2 on the progression of lung cancer in vitro and vivo. Results showed that H_2 inhibited cell viability, migration and invasion, and catalyzed cell apoptosis and H_2 induced A549 and H1975 cells G2/M arrest. Besides, H_2 down-regulated the expression of NIBPL, SMC3, SMC5 and SMC6, and also reduced the expression of Cyclin D1, CDK4 and CDK6. H_2 translocated the subcellular location of SMC3 during cell division and decreased its stability and increased its ubiquitination in both A549 and H1975 cells. In addition, inhibition of the proliferation, migration and invasion and promotion of the apoptosis of A549 and H1975 cells induced by H_2 were all abolished when overexpressed SMC3 in the presence of H_2. Animal experimental assay demonstrated that the tumor weight in H_2 group was significantly smaller than that in control group, but was bigger than cis-platinum group. The expression of Ki-67, VEGF and SMC3 were decreased when mice were treated with H_2 or cis-platinum, especially for cis-platinum. All data suggested that H_2 inhibited lung cancer progression through down-regulating SMC3, a regulator for chromosome condensation, which provided a new method for the treatment of lung cancer.

1. Introduction

Lung cancer is one of the most common lethal malignancies and lung adenocarcinoma accounts for more than 80% [1]. Based on the different pathological classifications, lung cancer can be divided into two major groups: small-cell lung cancer (SCLC) and non-small-cell lung cancer (NSCLC). NSCLC is a cancer of epithelial origin which is made up of several histological subtypes that differ in their cytology, embryonic origin, anatomical location, and oncogene expression [2]. Although, advanced improvements were paid to the diagnosis of and therapy for lung cancer, more than 80% of NSCLC display high metastatic potential and drug resistance, resulting in poor outcomes. Therefore, new therapeutic strategies are urgently needed for patients with lung cancer.

It's reported that hydrogen molecules can diffuse directly into tissues through cell membranes due to their small molecular weight, thereby exerting antioxidant, anti-inflammatory and antiapoptotic properties [3]. Hydrogen has mild reductive productivity, which is beneficial to avoiding serious toxicity side effects in medical procedures and there is no toxicity in itself. Recently, the therapeutic efficacy of H_2 supplementation has been applied into treatment of many kinds of diseases, including brain [4], heart [5], intestine [6] and lung [6], all with a better outcome. In lung transplantation studies, Kawamura et al. [7] and Coworkers [8] showed that treatment of the donor and recipient with inhaled hydrogen at a safe concentration (2%) improves lung functions by reducing oxidative stress in rats. Additionally, Diao et al. [9] reported that H_2 inhalation could attenuate sea water instillation-induced acute lung injury through ameliorating hypoxemia, reducing inflammatory events, alleviating the extent of oxidative injury, and inhibiting lung cell apoptosis in rabbits. However, whether H_2 exerts role in improving patients with lung cancer remains unknown.

Chromosome condensation, a rapid increase in chromatin compaction during mitosis, is essential process for establish mitotic chromosome organization and is induced at the initial phase [10], and plays pivotal roles in the faithful distribution of identical genetic material between daughter cells during mitosis. Condensin, a highly conserved protein complex from yeast to vertebrate, plays crucial roles for chromosomal condensation [11]. The eukaryotic SMC (structural

---

maintenance of chromosomes) proteins form two kinds of hetero-dimers: the SMC1-SMC3 and the SMC2-SMC4 types. These hetero-dimers constitute an essential part of higher order complexes, which are involved in chromatin and DNA dynamics. The two most prominent and best characterized complexes are cohesin and condensin, necessary for sister chromatid cohesion and chromosome condensation [12]. In vertebrates, two types of condensin, condensin I and condensin II, have been discovered. A condensin complex forms pentamer and the SMC2-SMC4 heterodimer is shared by condensin I and II as a core component. By contrast, the three non-SMC subunits are composed of different proteins: CAP-H, CAP-G, andCAP-D2 for condensin I; and CAP-H2, CAP-G2, and CAP-D3 for condensin II. Until now, study related to the function of chromosome condensation on cancer development, including lung cancer, is rare.

In the present study, we aimed to explore the function of H_2 and chromosome condensation on lung cancer. Firstly, we determined the function of H_2 on cell variety, apoptosis, cycle, migration and invasion, hoping to verify the antitumor roles of H_2. Then, we used RNA-seq, qRT-PCR and western blotting to detect the DEGs between H_2 group and control group with the objective that was to find the gene related to chromosome condensation. Finally, we confirmed the chromosome condensation and H_2 on the progression of lung cancer in vitro and vivo.

2. Materials and methods

2.1. Cell culture and H_2 treatment

Human lung cancer cell lines A549 and H1975 cells and normal lung cell line BEAS-2B were purchased from the American Type Culture Collection (ATCC; Manassas, VA, USA). A549 and BEAS-2B cells were cultured in DMEM medium or without high glucose (GIBCO, USA) and H1975 cells was cultured in RPMI-1640, all with 10% of fetal bovine serum (FBS; GIBCO, USA) in an atmosphere of 5% CO_2 at 37 °C. 25 cm² culture flasks were selected and all cells were harvested in a solution of trypsin-EDTA at the logarithmic growth phase (GIBCO, USA). For H_2 treatment, (Hydrogen machine; Huimei, China) cells were cultured in 20%, 40%, 60% and 80% H_2 for indicated times according to different experiments, and 5% CO_2 as its control (CK group).

2.2. RNA extraction and real-time PCR

Total RNA was extracted with TRIzol reagent (Life Technologies, USA) according to the manufacturer's instruction. RNA was then converted into cDNA performed with the PrimeScript 1 st Strand cDNA Synthesis Kit (Takara, Tokyo, Japan) and SYBR Premix Ex Taq (Takara, Tokyo, Japan) was used for mRNA expression detection, according to the manufacturer's protocols. Results were expressed using the relative quantification ($2^{-\Delta\Delta Ct}$) method. Primers sequences for qRT-PCR purchased from Invitrogen were as follows:

NIBPL (human)-F: ACGGAGTTGGCAGCACAGAT,
NIBPL (human)-R: CATCACGGCGCTTAGCCTCA;
SMC2 (human)-F: TCAGCAAACTGAGGTACAATCCCA,
SMC2 (human)-R: AGGCTGAGGCAGGAGAATCG;
SMC3 (human)-F: CAGCAAACTGAGGTACAATCCCA,
SMC3 (human)-R: CCGATGGCTGACTTGGTCAC;
SMC4 (human)-F: ATACTGAGAAAGAGGTGGATGA,
SMC4 (human)-R: TGAAGCAGATTGCGATGTT;
SMC5 (human)-F: ATCTCGGCCCACTGCAACTT,
SMC5 (human)-R: GCCCGGACGACAGTATGACA;
SMC6 (human)-F: TCTGCCTCCTGGGTTCAAGC,
SMC6 (human)-R: CGAGGCCAAGGTGGATGGAT;
GAPDH (human)-F: AGTCAGCTCTCTCCTTTCAGG,
GAPDH (human)-R: TCCACCACCCTGTTGCTGTA.

2.3. RNA library preparation and sequencing

A549 and H1975 cells with H_2 treatment or not were completely ground and total RNA was extracted using TRIzol (Invitrogen, Carlsbad, CA, USA) and was purified using DNase I [13,14]. A total amount of 3 µg RNA per sample was used as input material for the RNA sample preparations. Sequencing libraries were generated using NEBNext® Ultra™ RNA LibraryPrep Kit for Illumina® (NEB, USA) according to manufacturer's instructions. Briefly, mRNA was extracted from total RNA using oligo (dT) magnetic beads and sheared into short fragments of about 200 bases. These fragmented mRNAs were then used as templates for cDNA synthesis. The cDNAs were then PCR amplified to complete the library. The cDNA library was sequenced using an Illumina HiSeq™ 2000 platform.

2.4. Analysis of RNA-Seq data

Raw RNA-Seq reads were processed through in-house perl scripts. Clean reads were obtained by removing reads containing low quality reads and/or adaptor sequences from raw reads [15], and mapped to the human genome (Susscrofa 10.2) using Top Hat software [16],allowing up to two base mismatches. The exon expression level was then calculated using the reads per kilobasesper million reads (RPKM) method [17].We considered the gene was expressed exclusively in one of the two groups, if its RPKM $\geq$ 0.3 in one group and < 0.3 in the other group. Differential expression analysis was performed using the Benjamini and Hochberg's approach for controlling the false discovery rate [18].Genes with an adjusted P value < 0.05 and| $\log_2$ fold changes | < 1 were assigned as DEGs.

2.5. Western blotting analysis

The total proteins were extracted from cells with different treatments. The supernatants of cells were collected after centrifuging at 12,000 g and 4 °C for 25 min. The protein concentration was measured by the bicin choninic acid (BCA) method (Thermo Fisher Scientific, USA).To determine the levels of protein expression, 20 µg proteins from each simple were separated by 10% SDS-PAGE and transferred to PVDF membranes, incubated with primary antibodies at 4 °C overnight, respectively, and detected using the SuperSignal Chemiluminescent HRP Substrate after incubation with peroxidase-conjugated secondary antibodies for 1 h at room temperature. The immune complexes were examined by ECL detection (Millipore, USA). For quantification, the western blotting bands were quantified by Image J software (National Institutes of Health) after background subtraction. The following antibodies were purchased from Abcam (USA): rabbit monoclonal to SMC2 (No. ab10399), rabbit polyclonal to SMC3 (No. ab128919), Rabbit polyclonal to SMC4 (No. ab17957), rabbit monoclonal to SMC5 (No. ab185373) and rabbit monoclonal to SMC5 (No. ab18039).

2.6. Examination of SMC3 ubiquitination by immunoprecipitation (IP)

Forty-eight hours after transfection, cells were washed three times in PBS, harvested by scraping, and centrifuged for 5 min at 1000 rpm. The pelleted cells were lysed at 4 °C in 300 µl of cell lysis buffer (50 mM Tris HCl pH = 8, 120 mM NaCl, 1% Nonidet P-40 (NP- 40), 2 mM EDTA, Protease Inhibitor Cocktail Tablets) for 30 min. The lysate was centrifuged at 14,000 rpm at 4 °C for 30 min, and the supernatants were combined with 10 µl of anti-SMC3 agarose beads and mixed overnight at 4 °C. The immune adsorbents were collected by centrifugation for 3 min at 3000 rpm and washed three times by re-suspension and centrifugation (3 min at 3000 rpm) in cell lysis buffer. The samples were eluted into 15 µl of SDS loading buffer and heated for 5 min at 100 °C and subjected to SDS–PAGE electrophoresis. After electrophoretic transfer onto PVDF membranes as described above, the membranes were incubated with Ub antibody and then with peroxidase-conjugated

secondary antibody for detection of immunoreactive bands.

2.7. Cell proliferation assay

Cell proliferation was determined with Cell Counting Kit-8 assay (CCK-8). Briefly, cells were plated in a 96-well plate at a density of 2×10^3 cells per well, then put it into incubator with 20%, 40% or 60% content of H_2 for 2 h a day, and incubated cells at 37 °C in a 5% CO_2 humidified environment. 10 μl CCK-8 regent and 90 μl cell culture medium were added and cells were returned to incubate for 3 h. Light absorbance at 450 nm was measured daily with a microplate reader. Experiments with triplicates were performed independently at least thrice.

2.8. Colony forming assay

A549 and H1975 cells were plated at 300 cells per 35 mm tissue culture dish and incubated for 2 weeks at 37 °C in a 5% CO_2 humidified environment. Colonies were then photographed and counted in 3th day, 7th day and 14th day, respectively. Experiments with duplicates were performed independently at least thrice.

2.9. Cell cycle analysis

Cell cycle analysis was performed as previously described [19]. In brief, cells were synchronized with serum free media for 12 h. Then A549 and H1975 cells were treated with 20%, 40%, 60% or 80% H_2 for 24 h, then the cells were collected and fixed in 70% ethanol overnight at −20 °C. The cells were then collected, treated with RNase A (100 ng/ml) for 30 min and stained with propidium iodide (PI; 50 ng/ml) for 15 min. Next, samples were analyzed for cell cycle distribution with a MoFlo XDP flow cytometer (Beckman Coulter). Data were analyzed using FlowJo software (Treestar Inc., Brea, CA, USA). Experiments with duplicates were performed independently at least thrice.

2.10. Cell migration and invasion assay

For cell migration detection, wound healing assay was performed. 2×10^5 A549 and H1974 cells were seeded in per well of 24-well plate and allowed to reach confluence. A single-scratch wound was introduced through the middle of each well with a sterile pipette tip. Cell migration across the margins was assessed and photographed after 24 h.

For cell invasion detection, transwell assay was performed using 24-well transwells (8 μm, BD, USA). A549 and H1975 cells were added to the upper chamber of each migration well in 200 μl FBS-free medium after incubator with 20%, 40%, 60% or 80% content of H_2 for 2 h, and 600 μl DMEM with 10% FBS was added to the lower part of the chamber and invasion was allowed to occur for 48 h. The cells on the filter surface were fixed with methanol, stained with crystal violet and photographed with a phase-contrast inverted microscope. Experiments with triplicates were performed independently at least thrice.

2.11. Immunofluorescence

A549 and H1975 cells grown on cover slips were washed three times with phosphate buffered saline (PBS) followed by fixation in cold methanol for 10 min, washed with PBST three times, and blocked for 1 h with 5% goat serum in PBS. 1% Triton treatment was used to increase cell membrane permeability after cell morphology return to normal. Cells then were incubated with a rabbit anti-human SMC3 antibody incubated overnight at 4 °C followed by red fluorescence-labeled goat anti-rabbit secondary antibody incubated for 30 min darkly and DAPI labeled nuclei dark for 10 min, the green and blue fluorescent were observed and photographed using fluorescence microscopy. Each immuneofluorescence assay was repeated at least thrice.

2.12. Assay of cytokine production of IL-1β, IL-8, IL-13 and TNF-α by ELISA

The levels of cytokine production of interleukin-1β (IL-1β), IL-8, IL-13 and tumor necrosis factorα (TNF-α) from lung cancer tissues was detected by ELISA respectively according to per instruction manual in the ELISA kit. The absorbance at 450 nm (A450) was obtained using a bichromatic microplate reader (BIO-TEK, USA).

2.13. Measurement of ROS production and antioxidant enzyme activities

For the assessment of oxygen species (ROS) production, tissue samples were washed with PBS, digested with 0.5% trypsin and 0.1% collagenase for 40 min, centrifuged at 600 rpm for 5 min and re-suspended in D-Hank's buffer.

The antioxidant enzyme activities were measured using an oxide dismutase (SOD) activity detection kit (Nanjing Jian cheng Bioengineer Institute, China) following the manufacturer instructions.

2.14. In vivo tumorigenesis

Animal study was performed according to previous study [20] and had been performed in accordance with the Helsinki Declaration. Male BALB/c-nude mice aged 4 weeks were used for human tumor xenograft model (supplied by the Shanghai Experimental Animal Center, Chinese Academy of Sciences, Shanghai, China). BALB/c mice treated under normal atmosphere (Normal group) or 60% H_2 were used to evaluate the safety of H_2. BALB/c mice implanted with 1×10^7 A549 cells were divided into 3 groups when the tumors were grown 3 to 4 mm in diameter and visible: H_2, cis-platinum and control groups. The H_2 mice were inhaled with 60% H_2 2 h every day, and mice in cis-platinum group were given cis-platinum intraperitoneal injection. The atmosphere served as a control of 60% H_2 and the same amount of saline as a control of cis-platinum. The treatments were kept for 4 weeks. Then, the lung tissues of the mice from different groups were carried out immunohistochemistry to determine the protein expression of VEGF, Ki67 and SMC3. The procedure of immunohistochemistry referred to previous study. Brifly, paraffin sections of tissues were sliced into sections of 4 μm thickness by a slicing machine, and then a routine 3-step immunohistochemical stain was used: sectioning, dewaxing and hydrating the tissues; incubation with 3% H_2O_2 at room temperature for 10 min; antigen retrieval with Tris-EDTA; sealing with 5% goat serum (diluted in PBS); incubating overnight at 4 °C with primary antibody; and then incubating with secondary antibody and rinsing with PBS. Chromogen 3, 3′-diaminobenzidinetetrachloride (DAB) (Serva, Heidelberg, Germany) was used as a substrate. The cell nucleus was dyed with Harri's hematoxylin solution. Then the tissues were taken photo at ×200 magnification.

2.15. Statistical analysis

All values are presented as the mean ± the standard deviation (SD). Data were evaluated using one-way analysis of variance to determine if differences between the groups. A P value < 0.05 was considered statistically significant.

3. Results

3.1. H_2 inhibits A549 and H1975cells growth, migration and invasion

To explore the function of H_2 on lung cancer, we investigated the effect of H_2 on the growth, apoptosis, clone formation, migration, invasion and cycle of A549 and H1975 cells, firstly. As shown in Fig. 1A, the IC50 of H_2 on normal lung cells BEAS-2B was 77.0 ± 1.36%, indicating that H_2 is relatively safe for normal lung cells. However, both A549 and H1975 cells' proliferation was significantly inhibited by H_2
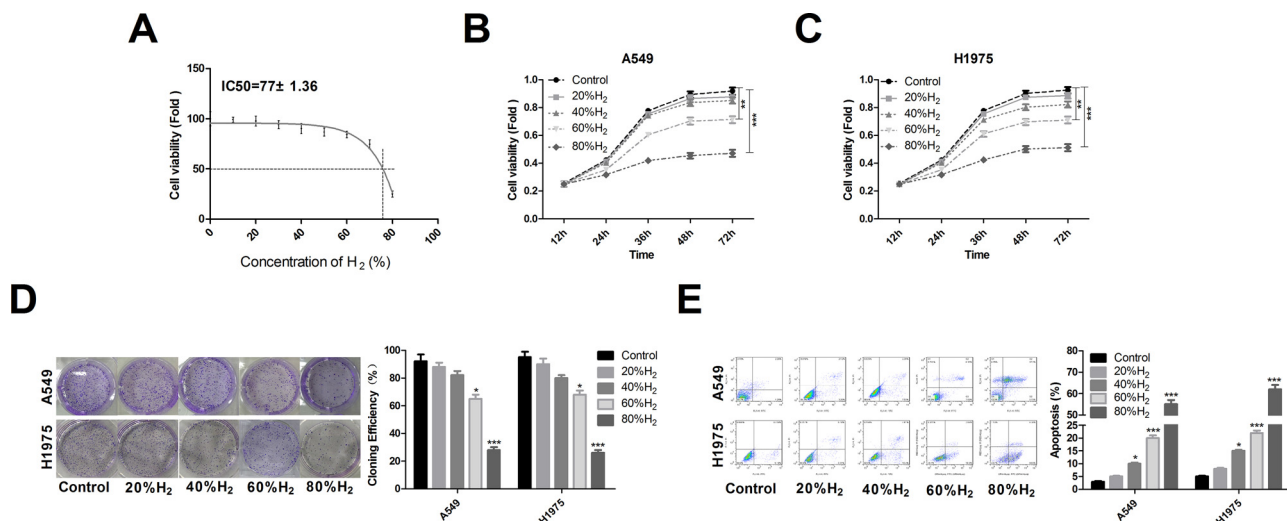
Fig. 1. H_2 function on A549 and H1975 cells growth and apoptosis. A) CCK-8 analysis the cell viability of normal lung cells BEAS-2B. B–C) Cell proliferation was detected by CCK-8 after A549 and H1975 cells were treated with 20% H_2, 40% H_2, 60% H_2 and 80% H_2 12 h, 24 h, 36 h, 48 h and 72 h. D) Colony forming assay was performed to test A549 and H1975 cells colony forming ability when cells were treated with 20% H_2, 40% H_2, 60% H_2 and 80% H_2 14 d, respectively. E) Cell apoptosis was detected by flow cytometry after A549 and H1975 cells were treated with 20% H_2, 40% H_2, 60% H_2 and 80% H_2 for 48 h, the percentage of early and late apoptotic cells was also analyzed by flow cytometric analysis of Annexin V/PI double staining. ($n = 3$, $^*P < 0.05$, $^{**}P < 0.01$, $^{***}P < 0.001$).
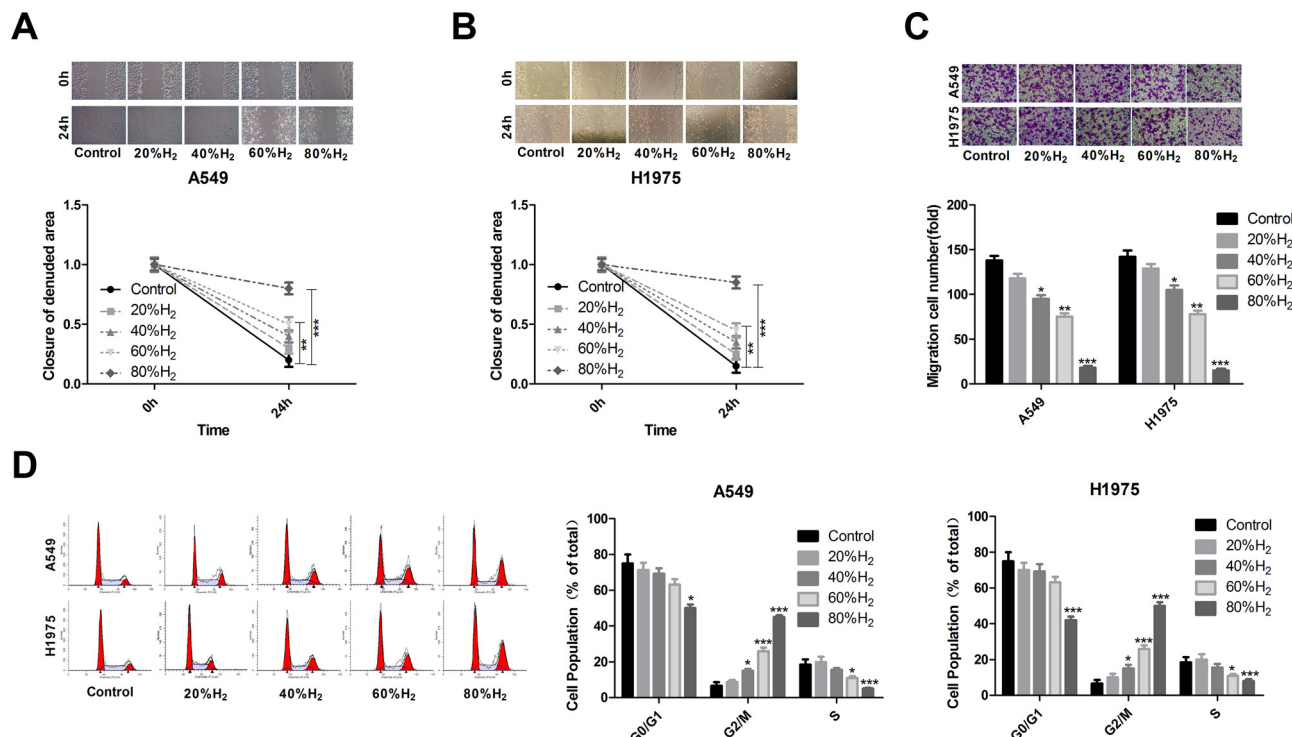
Fig. 2. H_2 function on A549 and H1975 cells' migration, invasion and cycle. A–B) Cell migration was determined by wound healing assay in A549 and H1975 cells treated with different treatments: control, 20% H_2, 40% H_2 60% H_2 and 80% H_2 groups. C) Cell invasion was examined by transwell assay in A549 and H1975 cells with various treatments. D) Flow cytometry was used to test cell cycle influenced by H_2 in A549 and H1975 cells. The bar graphs were on behalf of the number of cells in different cycle phases, which showed by mean ± SD. ($n = 3$, $^*P < 0.05$, $^{**}P < 0.01$, $^{***}P < 0.001$).

with a concentration of 60% and 80%, while there were no obviously change when the concentration of H_2 is 20% or 40% (Fig. 1B–C). The colony forming ability of A549 and H1975 cells was significantly impaired when cells were treated with 60% and 80% H_2 after 14 days, especially in 80% H_2 group (Fig. 1D). Flow cytometry showed that the apoptosis of A549 and H1975 cells was promoted when cells were treated with 60% and 80% H_2, and 80% H_2 showed rapid apoptosis (Fig. 1E), suggesting that 80% H_2 caused a serious damage to the cell, which wasn't safe to use. We also carried out wound healing and

transwell assays to detect the migration and invasion of H1975 and A549 cells in the presence of H_2. Results showed that the migration ability was reduced in the presence of 60% H_2 and 80% H_2 in both A549 (Fig. 2A) and H1975 cells (Fig. 2B). The invasion results demonstrated that 40%, 60% and 80% H_2 all could suppress A549 and H1975 cells' invasion significantly, especially in 80% H_2 group (Fig. 2C). Additionally, we examined the effects of H_2 on cell cycle through flow cytometry assay and we observed that H_2 promoted A549 and H1975 cells with G2/M arrest (Fig. 2D). All data illustrated that H_2
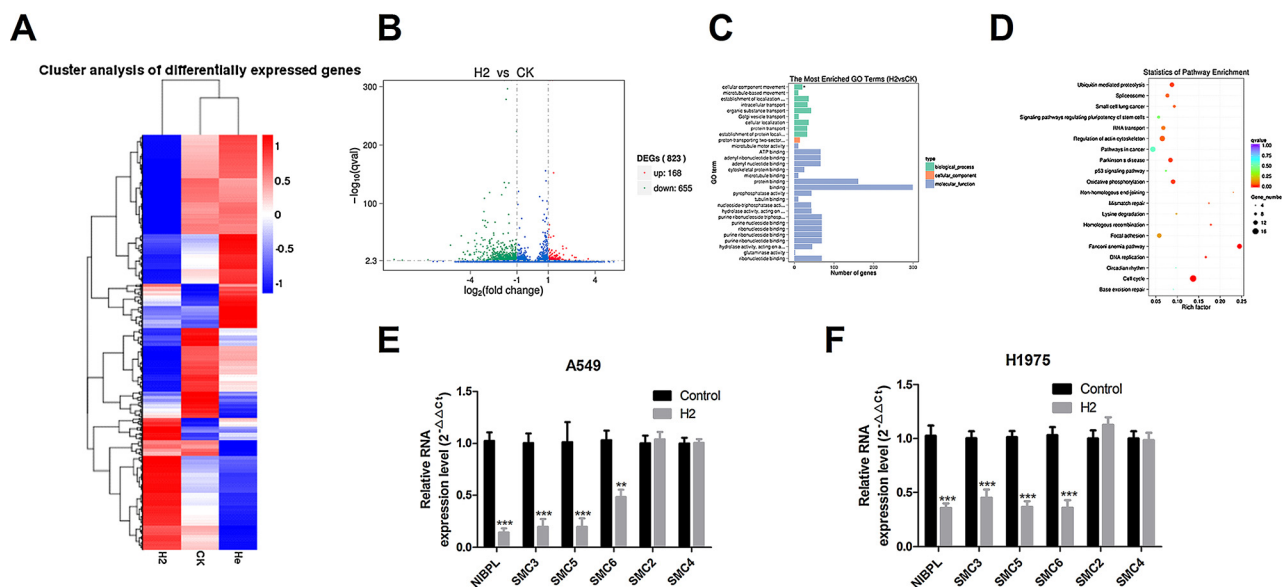
Fig. 3. The DEGs between H_2 and control groups were decided by RNA-seq method or qPCR. A) The heatmap of DEGs in A549 cells of H_2 and control groups. B) Volcano plot of DEGs in A549 cells treated with H_2 or not. C–D) The pathway analysis of the cell movement between H_2 and control groups. E–F) The mRNA levels of NIBPL, SMC2, SMC3, SMC4, SMC5 and SMC6 were detected by qPCR in A549 and H1975 cells. The bar graphs were on behalf of mean ± SD. (n = 3, $^*P < 0.05$, $^{**}P < 0.01$, $^{***}P < 0.001$).

inhibited lung cancer cell lines A549 and H1975 growth, migration and invasion, regulated cell cycle with G2/M arresting and promoted cell apoptosis, suggesting H_2 might play crucial roles in the treatment of lung cancer.

3.2. H_2 down-regulates the expression levels of NIBPL, SMC3, SMC5 and SMC6 in A549 and H1975 cells

To further investigate the potential molecular mechanisms of H_2 on lung cancer cells function, RNA-seq method and qPCR were used to search the DEGs between H_2 group and control groups (CK: 5% CO_2) in A549 cells. We adopted 60% H_2 for the next study. As shown in Fig. 3A and B, heatmap and volcano plot revealed the DEGs of H_2 and control groups in A549 cells. A total of 823 genes were differentially expressed between the two groups, in which 168 genes were upregulated and 655 genes were downregulated in the H_2 group. Table 1 listed the top 10 DEGs between the two groups. Besides, the pathways related to celluar component movement and cell division showed significantly difference between H_2 and CK group (Fig. 3C and D). Then to confirm the DEGs, we carried out qPCR to detected the mRNA levels of NIBPL, SMC2, SMC3, SMC4, SMC5 and SMC6, results displayed that the mRNA levels of NIBPL, SMC3, SMC5 and SMC6 were significantly decreased in H_2 group, when compared with control group, but the mRNA levels of SMC2 and SMC4 had no marked change between the two groups in both

A549 and H1975 cells (Fig. 3E and F). This part of results elucidated that H_2 down-regulated the expression levels of NIBPL, SMC3, SMC5 and SMC6 in lung cancer cell lines A549 and H1975. In addition, we also assessed the protein levels of NIBPL, SMC2, SMC3, SMC4, SMC5 and SMC6 and the subcellular location of SMC3. As shown in Fig. 4A and B, the protein levels of NIBPL, SMC3, SMC5 and SMC6 were significantly decreased in H_2 group, and the protein levels of SMC2 and SMC4 had no marked change when compared with CK group in both A549 and H1975 cells. And SMC3 showed the most obvious reduced trend after cells were treated with H_2, hence SMC3 was chose for our next study.

3.3. H_2 regulates SMC3 expression in mitotic period

Previous studies reported that SMC family plays pivotal roles in the maintenance of chromosomes, which is nuclear located in interphase and disappears from chromosomes in anaphase [21,22].To determine whether H_2 involved in chromosome condensation process, the immunofluorescence assay was performed to evaluate the subcellular location of SMC3. Fig. 4C and D displayed the change procedure of SMC3 expression during cell division of A549 and H1975 cells: the expression of SMC3 was weak in both control group and H_2 group in 0 h condition, where most cells were at static period; the expression of SMC3 was significantly higher than that in 0 h in both groups in 6 h condition,

Table 1
The 10 DEGs between CK and H_2 group.

Gene Name	P value	log2.Fold_change	readcount_H2	Read count_CK	Description
SMC3	1.65E-52	−2.5002	61.76719285	349.4520617	structural maintenance of chromosomes 3
NIPBL	1.76E-13	−2.2396	19.54070625	92.28296507	Nipped-B homolog (Drosophila)
SMC2	1.25E-34	−2.7549	30.31645192	204.6403111	structural maintenance of chromosomes 2
SMC4	1.07E-74	−3.1906	43.41233421	396.3580477	structural maintenance of chromosomes 4
SMC5	2.70E-15	−2.5483	15.72537047	91.98702825	structural maintenance of chromosomes 5
SMC6	1.26E-24	−2.5595	26.0886474	153.7885009	structural maintenance of chromosomes 6
CCDC41	0.00012151	−2.3541	4.640273252	23.72426841	coiled-coil domain containing 41
BRCC3	4.46E-08	−1.7773	19.79849921	67.86817741	BRCA1/BRCA2-containing complex, subunit 3
CENPJ	3.27E-06	−1.8433	13.0443237	46.80734038	centromere protein J
AKAP9	1.02E-35	−4.1406	8.713401996	153.6898552	A kinase (PRKA) anchor protein (yotiao) 9
CCDC18	1.54E-07	−4.7133	0	25.69718055	coiled-coil domain containing 18
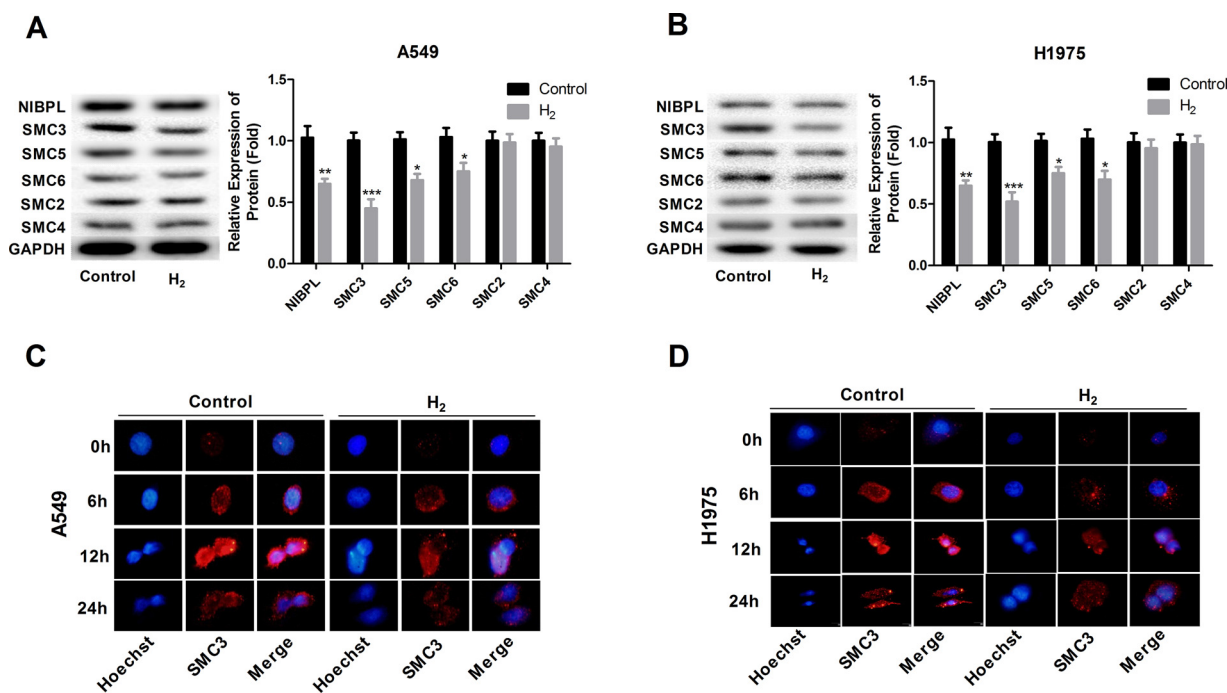
Fig. 4. The protein levels of SMC2/3/4/5/6 and NIBPL in A549 and H1975 cells. A–B) The protein expressions of SMC2/3/4/5/6 and NIBPL in A549 and H1975 cells in different groups: H_2 group and control group, were determined by western blotting analysis. C–D) The immunofluorescence assay was performed to test the subcellular location of SMC3 in A549 and H1975 cells. The bar graphs were on behalf of mean ± SD. (n = 3, [*], [#]$P < 0.05$, [**], [##]$P < 0.01$, [***], [###]$P < 0.001$).

with most cells were in a single cell nucleus, but the expression of SMC3 was significantly lower in H_2 group than that in control group; In 12 h condition, most cells might be in cell division and had double nucleus, in which the SMC3 expression was very high but H_2 group was lower than control group; In 24 h condition, cell has been divided into two cells, and the expression of SMC3 had begun to decrease. In the same period, SMC3 protein expression in H_2 group was less than that in the CK group (Fig. 4C and D), which was consistent with the results from western blotting and qPCR. According to the change of SMC3 expression in a cell cycle, we also evaluated the expression of proteins related to cell cycle, such as cyclin D1, CDK4 and CDK6 influenced by H_2. Compared with the control group, H_2 decreased the expression of cyclin D1, CDK4 and CDK6 in both A549 (Fig. 5A) and H1975 cells (Fig. 5B). In addition, we used CHX to detect the stability of SMC3 protein in the presence of H_2, results showed that H_2 decreased the stability of SMC3 protein in both A549 (Fig. 6A) and H1975 cells (Fig. 6C). And the IP assay demonstrated that H_2 reduced SMC3 protein expression through promoting its ubiquitination (Fig. 6B and D). All data suggested that H_2 down-regulated SMC3 expression in lung cancer cell lines.

3.4. H_2 inhibits the proliferation and promotes the apoptosis of A549 and H1975 cells through down-regulating SMC3 expression

Next, we explored the function of SMC3 in the progression of lung cancer in the presence of H_2. Fig. 6A and B showed the transfected efficiencies of over-expressed SMC3 vector (OE-SMC3) in both A549 and H1975 cells by using qPCR and western blotting, and both the mRNA and protein expression levels of SMC3 were significantly elevated when A549 and H1975 cells were transfected OE-SMC3, as compared with the control group (Fig. 7A and B). Would healing and transwell assays demonstrated that the inhibition of the migration and invasion of A549 and H1975 cells induced by H_2 were abolished when overexpressed SMC3 in the presence of H_2 (Fig. 7C and E). Besides, the promotion of cell apoptosis induced by H_2 was also impaired when overexpressed SMC3 in the presence of H_2 in both A549 and H1975 cells (Fig. 7F). These results illustrated that H_2 inhibited cell

proliferation, migration and invasion and promoted cell apoptosis through down-regulating SMC3 expression in lung cancer cells.

3.5. H_2 inhibits tumorigenesis in vivo

It's well known that cis-platinum is an antitumor drug, which is widely used to the patients with lung cancer. Our study manifested that H_2 could also play an antitumor effect in lung cancer according to the above experiments results, which exerted inhibiting cell variety and promoting cell apoptosis roles in lung cancer cell line A549 and H1975 cells. Therefore, we compared the anticancer role of cis-platinum and H_2 in vivo. We divided the 50 nude mice into Normal group (mice without xenograft under normal conditions), Normal + H_2 group, xenograft group, H_2 + xenograft group and cis-platinum + xenograft group, with each group 10 mice. The BALB/c mice were implanted with 1×10^7 A549 cells and the mice in H_2 group were inhaled with 60% H_2 2 h every day, while the mice in cis-platinum group were given intraperitoneal injection cis-platinum resolved in saline solution according to 4 mg/kg every 5 day. The treatments were kept for 4 weeks, then we took out the tumor and weighed the weight of every mouse. As shown in Fig. 8A, the hematoxylin-eosin (HE) staining indicated that H_2 showed no significantly impact on normal mice lung tissues as compared with the control group, and both H_2 and cis-platinum could reverse the pathological lung tissues into approximately normal. Immunohistochemistry was performed to detect the expression of Ki-67, an index indicating cell proliferation, as well as VEGF and SMC3, which showed that the protein expression levels of Ki-67, VEGF and SMC3 showed no significantly change between Normal group and Normal + H_2 group, and the protein expression of Ki-67, VEGF and SMC3 were all reduced in H_2 and cis-platinum groups (Fig. 8B). In addition, the levels of ROS, SOD and pro-inflammatory factors such as IL-1β, IL-8, IL-13 and TNF-α were all showed no obvious change among Normal group and Normal + H_2 group (Fig. 8D–F). And the ROS level was reduced and SOD level was increased when treated the tumor-bearing mice with H_2 and cis-platinum (Fig. 8D–F), and the levels of pro-inflammatory factors such as IL-1β, IL-8, IL-13 and TNF-α were all reduced (Fig. 8F). Furthermore, the weights of tumor in either H_2 group or cis-platinum
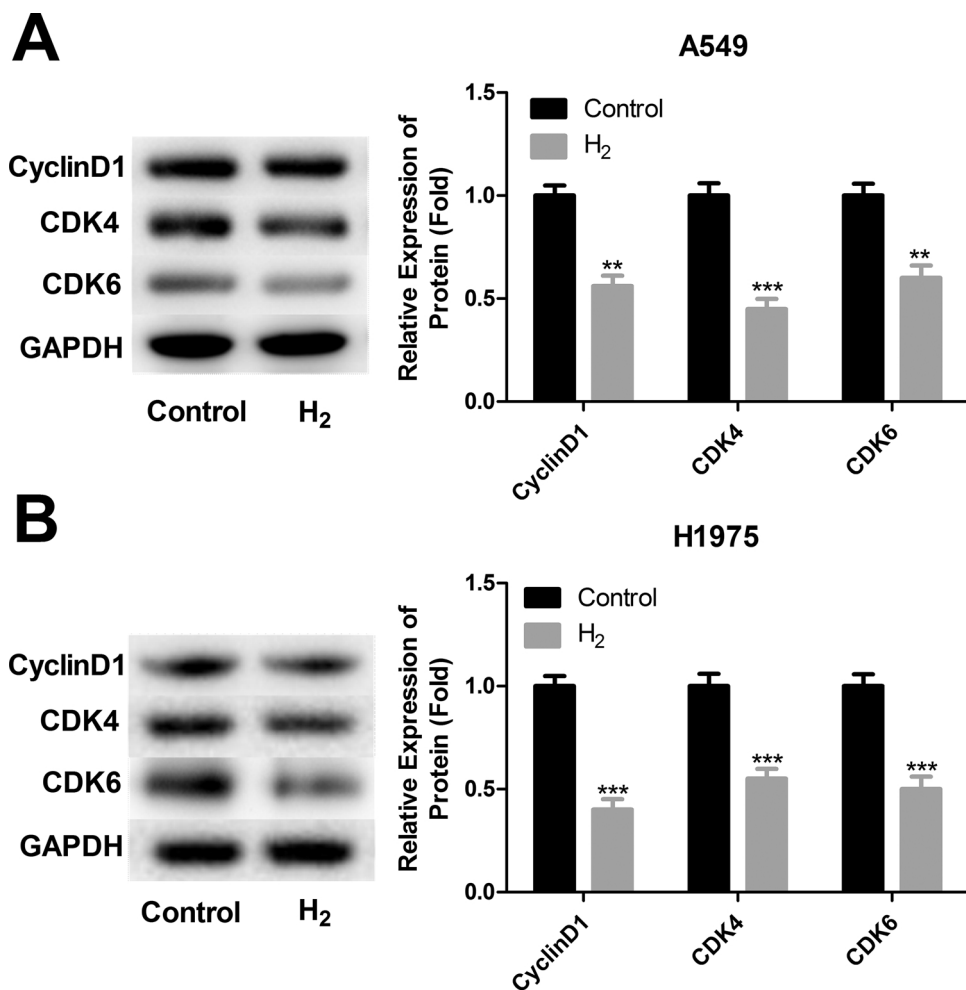
Fig. 5. The protein levels of Cyclin D1, CDK4 and CDK6 in A549 and H1975 cells. A–B) Western blotting analysis of the effect of H_2 on the expression levels of Cyclin D1, CDK4 and CDK6 in A549 and H1975 cells. The bar graphs were on behalf of mean ± SD. (n = 3, [*, #]$P < 0.05$, [**, ##]$P < 0.01$, [***, ###]$P < 0.001$).
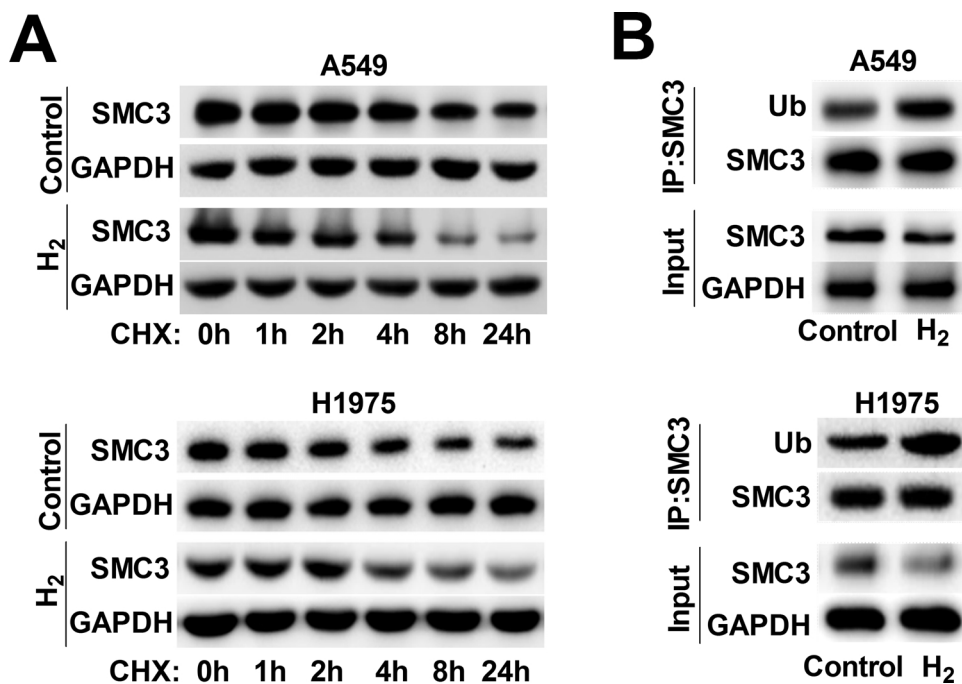
Fig. 6. The effects of H_2 on the stability and ubiquitination of SMC3. A) H1975 and A549 cells were treated with 60% H_2 for 24 h. Cells were then treated with CHX (100 μg/ml) for the 1, 2, 4, 8, 24 h, and western blotting was performed. B) IP assay was used to assess the expression of ubiquitination protein (Ub) combining with SMC3 in the presence of H_2.
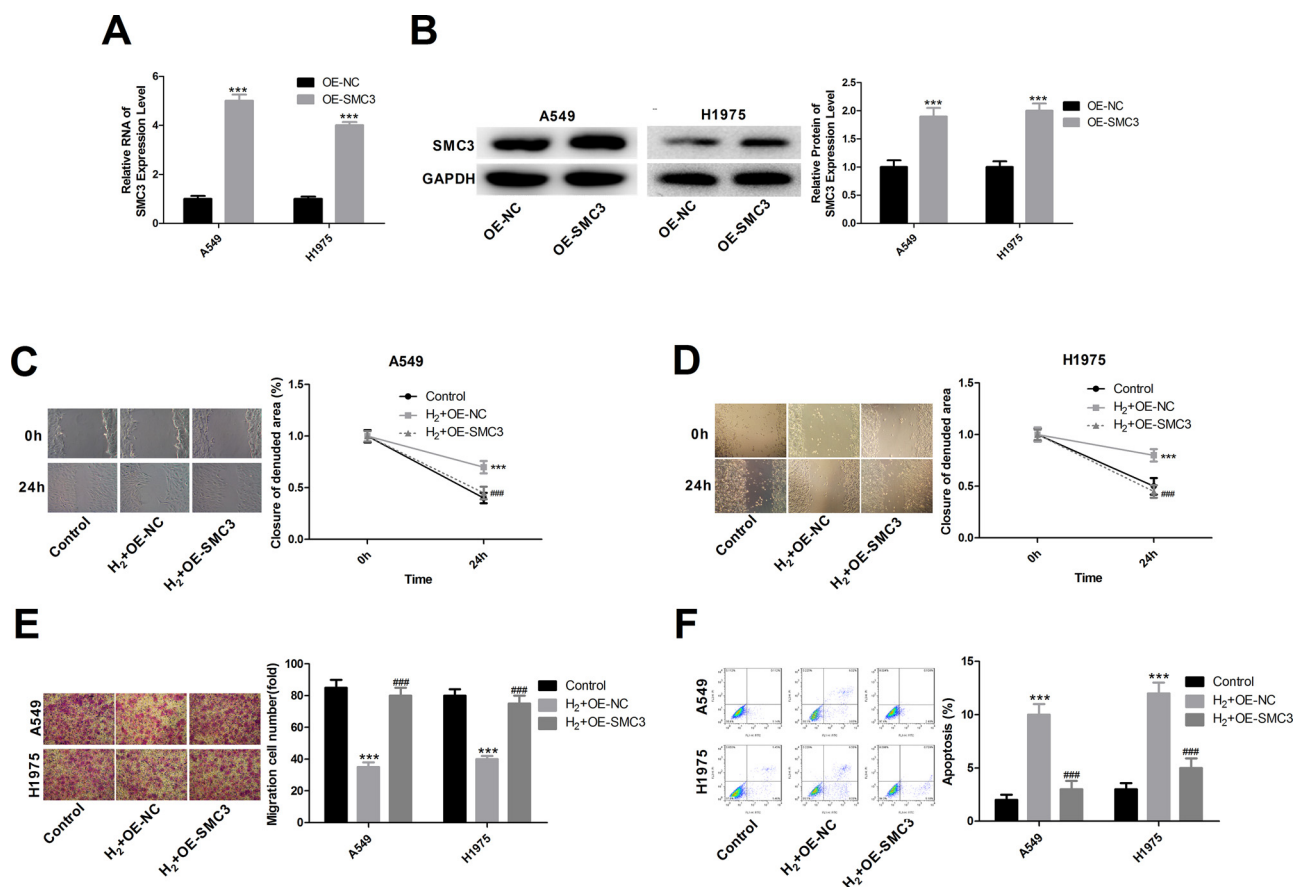
Fig. 7. The effects of H2/SMC3 on the proliferation, migration, invasion and apoptosis of A549 and H1975 cells. A–B) QPCR and western blotting were performed to detect the transfected efficiency of OE-SMC3 in A549 and H1975 cells. C-D) Wound healing assay was performed to evaluate the effect of H_2/SMC3 in the migration of A549 and H1975 cells. E) Transwell assay was performed to evaluate the effect of H_2/SMC3 in the invasion of A549 and H1975 cells. F) Flow cytometry assay was performed to evaluate the effect of H_2/SMC3 on the apoptosis of A549 and H1975 cells. The bar graphs were on behalf of mean ± SD. (n = 3, [*], [#]$P < 0.05$, [**], [##]$P < 0.01$, [***], [###]$P < 0.001$).

group were significant less than that in control group, however, the anticancer role induced by H_2 showed no better than cis-platinum (Fig. 8C). All data suggested that H_2 inhibited the carcinogenesis in lung cancer, and also exerted anti-oxidant and inflammatory roles, but its curative effect was not better than cis-platinum.

4. Discussion

Metastasis is the major factor associated with poor prognosis of lung carcinoma, and lymph node metastasis is an important way [23].The current study showed that H_2, a colorless, odorless, and tasteless gas, inhibited lung cancer cells A549 and H1975 viability, migration and invasion through down-regulating SMC3 expression, and exerted no significantly impact on normal animals, indicating H_2 might serve as a therapeutic method and play anti-tumor roles in cancer.

Recently, many studies have verified gas might exert an anti-cancer effect or play a crucial role in fighting diseases, which attract broad attention based on low incidence of side effects [24,25]. Among the gasotransmitter family, nitric oxide (NO) serves as a "star" messenger involved in a number of physiological and pathological activities [26]. Especially in the field of cancer therapy, NO not only directly kills cancerous cells at high concentrations (> 1 mm) through the nitrosation of mitochondria and DNA [27], but also cooperatively enhances the efficacy of photodynamic therapy or radiotherapy [28]. Additionally, scientists have initially found that high-pressure hydrogen exerted anti-inflammatory effects by reacting with hydroxyl-free radicals directly in 2001 [29]. But the molecular mechanism of H_2 in lung cancer is rarely studied. From the RNA-seq and qRT-PCR results of our

study, the genes encoding proteins that related to chromosome condensation showed significantly difference among H_2 group and control group, including NIPBL, SMC3, SMC5 and SMC6, which were down-regulated in H_2 group compared with that in control group, suggesting that chromosome condensation maybe involve in the antitumor progress induced by H_2 in lung cancer. Additionally, previous study reported that, heterozygous mutations in the NIPBL, RAD21, and SMC3 genes are transmitted in an autosomal dominant pattern [30], illustrating that the mutations of SMC3 and NIPBL might occur in lung cancer patients, but this hypothesis need to be further verified in our next study.

Throughout all kingdoms of life, SMC proteins are responsible for the faithful inheritance of genetic information. They are involved in a wide range of vital cellular processes from cell division to gene regulation and DNA repair, acting as global organizers and safeguards of the genome. Where prokaryotic genomes encode for only one SMC protein that exists as a homodimer, and there are six different SMC proteins that form three distinct heterodimeric complexes in eukaryotes, with the holo complexes additionally containing several specific regulatory non-SMC subunits [31]. In eukaryotes, the complex containing SMC1 and SMC3, named cohesin, is responsible for sister chromatid cohesion during mitosis and meiosis [32]. The condensin complex with SMC2 and SMC4 at its core is required, but not solely responsible for proper chromosome condensation and segregation during cell division [33]. It seems to organize and maintain the chromosome scaffold rather than actually establishing it [34]. And the unnamed SMC5–SMC6 complex is involved in several DNA repair pathways as well as homologous recombination in meiosis [35]. In the
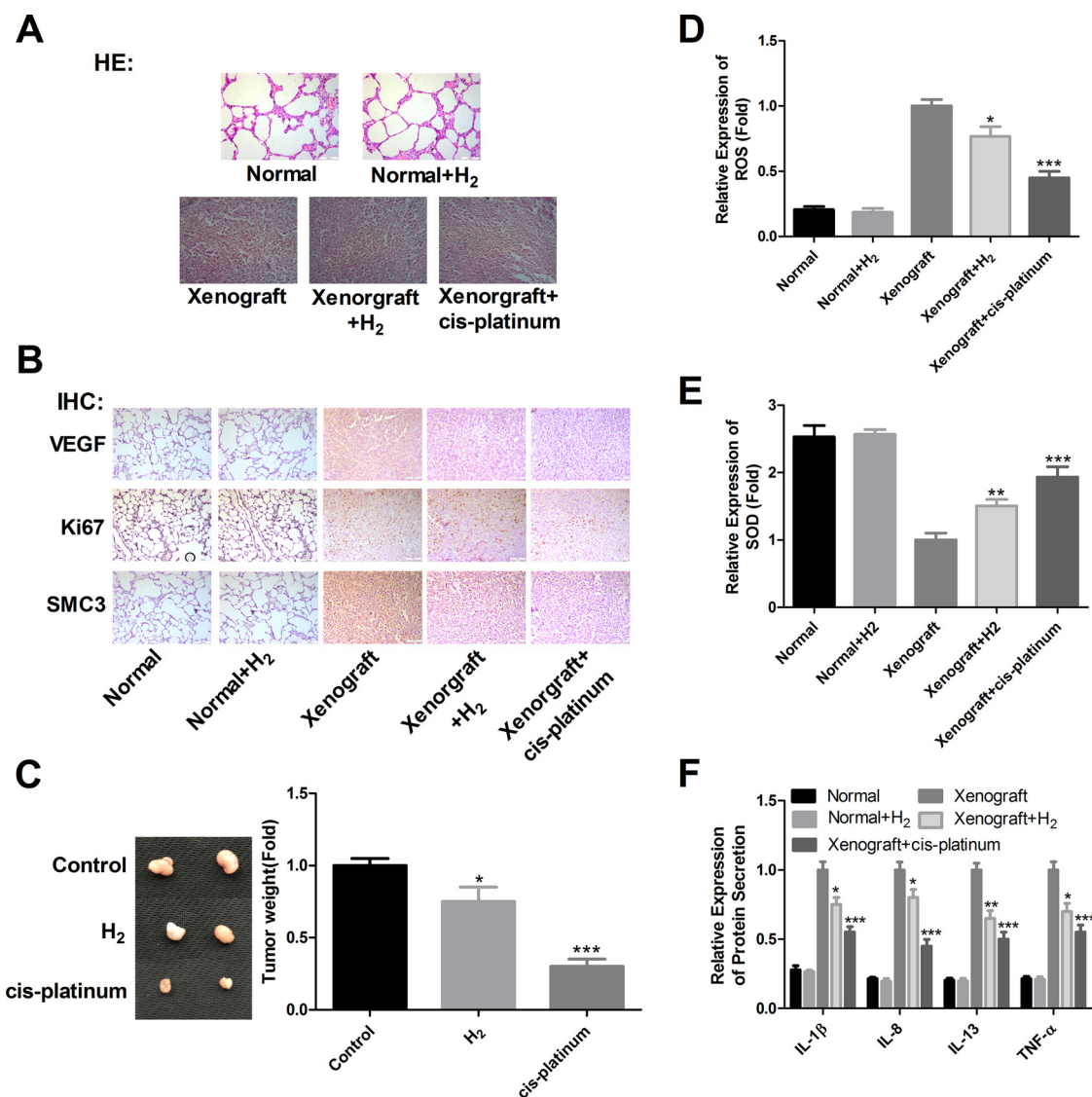
Fig. 8. H_2 inhibits tumorigenesis in vivo. A) HE staining was performed to test the pathological morphology of lung cancer tissues. B) Immunohistochemistry was used to detect the expression of Ki-67, VEGF and SMC3. C) The weights of tumors from mice with different treatment. D–E) The effects of H_2 and cis-platinum on the levels of ROS and SOD tumor-bearing mice. F) ELISA analysis of the serum IL-1β, IL-8, IL-13 and TNF-α. The bar graphs were on behalf of mean ± SD. (n = 10, $^*P < 0.05$, $^{***}P < 0.001$).

present study, we found that the mRNA and protein levels of SMC3, SMC5 and SMC6, but not SMC2 and SMC4 was reduced significantly when cells were treated with H_2. SMC3, as a cohesin, which is a multi-subunit protein complex involved in chromosome organization, is frequently mutated or aberrantly expressed in many kinds of cancer, with particularly high frequency in acute myeloid leukemia [36–38]. The SMC3 subunit of cohesin is acetylated (ac) during S phase to establish cohesion between replicated chromosomes. In the present study, we observed a G2/M delay of H_2, which was possible caused by accumulated ac-SMC3 [39]. In addition, we observed that the over-expression of SMC3 abolished the promotion of apoptosis and inhibition of the proliferation, migration and invasion induced by H_2. Besides, we carried out xenograft model to detect the expression of Ki-67, VEGF and SMC3, as well as compare the therapeutic effect of H_2 with cis-platinum. We observed that the weight of tumor and the protein expression of Ki-67, VEGF and SMC3 were all reduced in H_2 and cis-platinum groups, particularly in cis-platinum group, indicating that H_2 played an antitumor effect in lung cancer, but its curative effect was not better than cis-platinum. H_2, as a green gas, is beneficial to avoiding serious toxicity side effects in medical procedures and there is no toxicity in

itself. Liu et al. [6] reported that, combined early fluid resuscitation and hydrogen inhalation attenuated lung and intestine injury. Additionally, Qiu et al. [40] found that hydrogen inhalation could ameliorate lipopolysaccharide-induced acute lung injury in mice. These previous studies all suggested that H_2 had effective treatment effect for lung injury, and our study, for the first time, clarified the function of H_2 on lung cancer.

Cohesin has crucial roles in cell division and gene expression, providing potential novel therapeutic target for cancer. The lack of chromosome abnormalities in many cancers with cohesin alterations raises the intriguing possibility that cohesin contributes to cancer through its role in transcription. This study manifested that H_2 had a cytostatic effect on lung cancer cell lines A549 and H1975 through down regulating SMC3 expression. But the molecular mechanisms of SMC3 on lung cancer occurrence and development still need to explore.

Conflict of interest

The authors declare that they have no conflict of interest.

Acknowledgements

References

[1] R. Siegel, D. Naishadham, A. Jemal, Cancer statistics, CA Cancer J. Clin. 62 (1) (2012) 10–29 2012.

[2] W.D. Travis, Pathology of lung cancer, Clin. Chest Med. 32 (4) (2011) 669–692.

[3] I. Ohsawa, et al., Hydrogen acts as a therapeutic antioxidant by selectively reducing cytotoxic oxygen radicals, Nat. Med. 13 (6) (2007) 688–694.

[4] J. Cai, et al., Neuroprotective effects of hydrogen saline in neonatal hypoxia-ischemia rat model, Brain Res. 1256 (2009) 129–137.

[5] K. Hayashida, et al., Inhalation of hydrogen gas reduces infarct size in the rat model of myocardial ischemia-reperfusion injury, Biochem. Biophys. Res. Commun. 373 (1) (2008) 30–35.

[6] W. Liu, et al., Combined early fluid resuscitation and hydrogen inhalation attenuates lung and intestine injury, World J. Gastroenterol. 19 (4) (2013) 492–502.

[7] T. Kawamura, et al., Inhaled hydrogen gas therapy for prevention of lung transplant-induced ischemia/reperfusion injury in rats, Transplantation 90 (12) (2010) 1344–1351.

[8] T. Kawamura, et al., The effect of donor treatment with hydrogen on lung allograft function in rats, Surgery 150 (2) (2011) 240–249.

[9] M. Diao, et al., Hydrogen gas inhalation attenuates seawater instillation-induced acute lung injury via the Nrf2 pathway in rabbits, Inflammation 39 (6) (2016) 2029–2039.

[10] Y. Kagami, M. Ono, K. Yoshida, Plk1 phosphorylation of CAP-H2 triggers chromosome condensation by condensin II at the early phase of mitosis, Sci. Rep. 7 (1) (2017) 5583.

[11] T. Hirano, Condensin-based chromosome organization from bacteria to vertebrates, Cell 164 (5) (2016) 847–857.

[12] A.V. Strunnikov, R. Jessberger, Structural maintenance of chromosomes (SMC) proteins: conserved molecular properties for multiple biological functions, Eur. J. Biochem. 263 (1) (1999) 6–13.

[13] M. Cioffi, et al., Identification of a distinct population of CD133 + CXCR4 + cancer stem cells in ovarian cancer, Sci. Rep. (2015) 5.

[14] X. Li, et al., Lyn regulates inflammatory responses in Klebsiella pneumoniae infection via the p38/NF-kappaB pathway, Eur. J. Immunol. 44 (3) (2014) 763–773.

[15] P. Kerpedjiev, et al., Adaptable probabilistic mapping of short reads using position specific scoring matrices, BMC Bioinform. 15 (2014) 100.

[16] D. Kim, S.L. Salzberg, TopHat-Fusion: an algorithm for discovery of novel fusion transcripts, Genome Biol. 12 (8) (2011) R72.

[17] A. Mortazavi, et al., Mapping and quantifying mammalian transcriptomes by RNA-Seq, Nat. Methods 5 (7) (2008) 621–628.

[18] Y. Benjamini, et al., Controlling the false discovery rate in behavior genetics research, Behav. Brain Res. 125 (1-2) (2001) 279–284.

[19] Y.L. Li, et al., MicroRNA-34a/EGFR axis plays pivotal roles in lung tumorigenesis, Oncogenesis 6 (8) (2017) e372.

[20] Y. Lin, et al., Cyclin-dependent kinase 4 is a novel target in micoRNA-195-mediated cell cycle arrest in bladder cancer cells, FEBS Lett. 586 (4) (2012) 442–447.

[21] J. Mascarenhas, et al., Cell cycle-dependent localization of two novel prokaryotic chromosome segregation and condensation proteins in Bacillus subtilis that interact with SMC protein, EMBO J. 21 (12) (2002) 3108–3118.

[22] T. Hirano, The ABCs of SMC proteins: two-armed ATPases for chromosome condensation, cohesion, and repair, Genes Dev. 16 (4) (2002) 399–414.

[23] V. Morales-Oyarvide, M. Mino-Kenudson, High-grade lung adenocarcinomas with micropapillary and/or solid patterns: a review, Curr. Opin. Pulm. Med. 20 (4) (2014) 317–323.

[24] J. Kang, et al., pH-controlled hydrogen sulfide release for myocardial ischemia-reperfusion injury, J. Am. Chem. Soc. 138 (20) (2016) 6336–6339.

[25] J. Gehring, et al., Sunlight-triggered nanoparticle synergy: teamwork of reactive oxygen species and nitric oxide released from mesoporous organosilica with advanced antibacterial activity, J. Am. Chem. Soc. 138 (9) (2016) 3076–3084.

[26] M.C. Frost, M.E. Meyerhoff, Controlled photoinitiated release of nitric oxide from polymer films containing S-nitroso-N-acetyl-DL-penicillamine derivatized fumed silica filler, J. Am. Chem. Soc. 126 (5) (2004) 1348–1349.

[27] J. Fan, et al., A novel self-assembled sandwich nanomedicine for NIR-responsive release of NO, Nanoscale 7 (47) (2015) 20055–20062.

[28] W. Fan, et al., X-ray radiation-controlled NO-release for on-demand depth-independent hypoxic radiosensitization, Angew. Chem. Int. Ed. Engl. 54 (47) (2015) 14026–14030.

[29] B. Gharib, et al., Anti-inflammatory properties of molecular hydrogen: investigation on parasite-induced liver inflammation, C R Acad. Sci. III 324 (8) (2001) 719–724.

[30] E. Infante, G. Alkorta-Aranburu, A. El-Gharbawy, Rare form of autosomal dominant familial Cornelia de Lange syndrome due to a novel duplication in SMC3, Clin. Case Rep. 5 (8) (2017) 1277–1283.

[31] T. Hirano, At the heart of the chromosome: SMC proteins in action, Nat. Rev. Mol. Cell. Biol. 7 (5) (2006) 311–322.

[32] K. Nasmyth, C.H. Haering, Cohesin: its roles and mechanisms, Annu. Rev. Genet. 43 (2009) 525–558.

[33] D.F. Hudson, K.M. Marshall, W.C. Earnshaw, Condensin: architect of mitotic chromosomes, Chromosome Res. 17 (2) (2009) 131–144.

[34] P. Vagnarelli, et al., Condensin and Repo-Man-PP1 co-operate in the regulation of chromosome architecture during mitosis, Nat. Cell Biol. 8 (10) (2006) 1133–1142.

[35] G. De Piccoli, J. Torres-Rosell, L. Aragon, The unnamed complex: what do we know about Smc5-Smc6? Chromosome Res. 17 (2) (2009) 251–263.

[36] A. Kon, et al., Recurrent mutations in multiple components of the cohesin complex in myeloid neoplasms, Nat. Genet. 45 (10) (2013) 1232–1237.

[37] M.D. Leiserson, et al., Pan-cancer network analysis identifies combinations of rare somatic mutations across pathways and protein complexes, Nat. Genet. 47 (2) (2015) 106–114.

[38] S. Thota, et al., Genetic alterations of the cohesin complex genes in myeloid malignancies, Blood 124 (11) (2014) 1790–1798.

[39] T. Dasgupta, et al., HDAC8 inhibition blocks SMC3 deacetylation and delays cell cycle progression without affecting cohesin-dependent transcription in MCF7 cancer cells, J. Biol. Chem. 291 (24) (2016) 12761–12770.

[40] X. Qiu, et al., Hydrogen inhalation ameliorates lipopolysaccharide-induced acute lung injury in mice, Int. Immunopharmacol. 11 (12) (2011) 2130–2137.